Circularly Polarized DRA Mounted on or Embedded in Conformal Surface

S.H. Zainud-Deen[1*], N.A. El-Shalaby[2] and K.H. Awadalla[1].
[1]Faculty of Electronic Eng., Menoufia University, Egypt,[*]anssaber@yahoo.com
[2]Kafer El-Sheikh University, Egypt, noha1511ahm @yahoo.com

Abstract- **In this paper, the effect of curvature on circular polarization (CP) radiation characteristics of circularly-polarized dielectric resonator antenna (DRA) mounted on or embedded in cylindrical surfaces are studied. The antenna is designed for wireless applications at 9 GHz. In order to eliminate the effect of ground plane curvature on the CP characteristics by varying the DRA element height or embedded the DRA element in the curvature structure. The analysis using the finite element method (FEM) is applied. The results are validated by comparing with that calculated by the finite integration technique (FIT).**

I. Introduction

In modern communication systems, DRA has been used due to their advantages including its small size, low loss, low cost, light weight, and ease of excitation [1]. In most of DRAs applications, circular polarization antennas are usually preferred. CP antennas are less sensitive to orientation of the transmitter and the receiver [2]. In addition, the CP antenna reduces the propagation loss between the transmitting and the receiving antennas [3-5]. Most of the work on the DRA theory and technology has been concentrated on the performance of the DRA on planar surfaces. However, placing antennas on conformal structures (cylindrical or spherical) plays a considerable role in modern communication systems such as spatial domain multiple access (SDMA), smart antennas, beam-steering array antennas and aerospace applications [6]. The effect of ground plane curvature on the radiation characteristics of a cylindrical DRA mounted on or embedded in a hollow cylindrical ground plane have been investigated in [7, 8]. The radiation characteristics of a hemispherical DRA mounted on or embedded in a spherical ground plane have been investigated in [9-11]. In this paper, the effect of changing the ground plane curvature on the circular polarization properties of the circularly-polarized DRA has been demonstrated. The antenna is mounted on or embedded in a cylindrical ground plane. The DRA elements are designed and analyzed using the finite element method (FEM) [12] and the results are compared with those obtained by the finite integral technique (FIT) [13].

II. Numerical Results

A) DRA Mounted on a Cylindrical Ground Plane

A circularly-polarized square DRA with truncated edges mounted on a planer ground plane using a single feeding probe was introduced in [6]. The circular polarization characteristics are produced due to the generation of two orthogonal modes in the antenna structure. The DRA has square cross section with dielectric constant ε_r =9.4, edge length a =7.5 mm, and height h=6 mm as shown in Fig.1a. Two triangles are removed from the two corners along one diagonal of the DRA with c= 3.125 mm. A coaxial probe with radius of 0.15 mm, and height h_f =3 mm located at d_f =3 mm is used to excite the antenna. DRA element is mounted on a hollow hemi-cylindrical ground plane with radius R_g= 15 mm, m_g=π R_g, and l_g = 60 mm as shown in Fig.1b. The simulated reflection coefficient against the frequency and the circular polarization radiation pattern components, left-hand E_L and right-hand E_R in x-z plane and y-z plane are calculated at resonance frequency 9.25 GHz for the DRA mounted on hemi-cylindrical ground plane are shown in Fig.2.

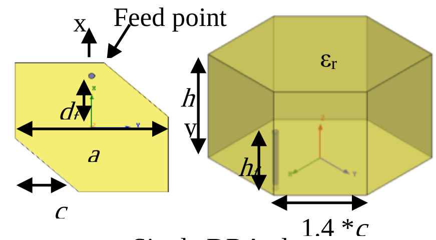

a. Single DRA element

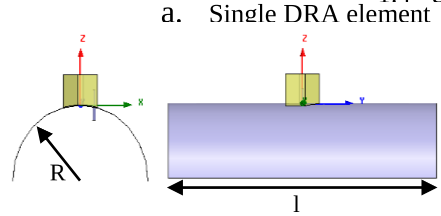

b. Geometry of DRA mounted on metallic hemi-cylindrical ground

Fig.1. The geometry of DRA element mounted on cylindrical ground plane.

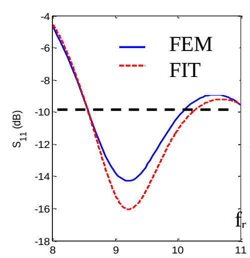

a. Reflection coefficient.

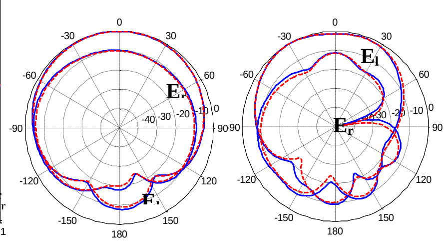

b. The polarization patterns of DRA.

Fig.2. Radiation characteristics of DRA mounted on hemi-cylindrical ground plane at f=9.25 GHz.

The impedance matching bandwidth with (S_{11}<-10dB) is 1.5 GHz for the curved ground plane case. The resonance frequency is shifted up for the curved ground plane case to 9.2 GHz due to the change in the size of the DRA to follow the curvature of the ground plane. Also, the change of the feed probe position inside the DRA will launch different modes with higher frequencies in the studied cases. The ratio of E_L/E_R is 9.8 dB for the curved case. The FEM method (solid line) is used to simulate the radiation characteristics of the DRA structure on different shapes of the ground plane and the results are compared with those determined using the FIT method (dotted line). Good agreement between the results of the two methods is obtained. Figure 3 shows the DRA element mounted on a hemi-cylindrical ground plane with different radii of curvature for a fixed physical area ($l_g \times m_g$). The effect of varying the radius of curvature R_g on the reflection coefficient and axial ratio of DRA are demonstrated in Fig.4. It is seen that the axial ratio is reduced with increasing the radius of the hemi-cylindrical ground plane. When R_g=60 mm, the antenna produces the minimum axial ratio at f= 9.25 GHz. The antenna has circular polarization bandwidth (AR<3 dB) over the frequency band from 9.1 GHz to 9.5 GHz within which the antenna matching is still preserved. The impedance matching is increased by increasing the radius of curvature. The resonance frequencies for different values of radius of curvature are decreased by increasing the radius of curvature of the ground plane. A comparison of different cases is presented in Table I.

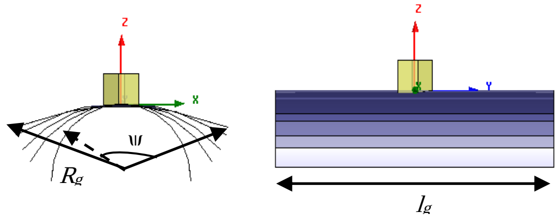

Fig.3. The geometry of DRA element mounted on a hemi-cylindrical ground plane with different radii for ground plane area.

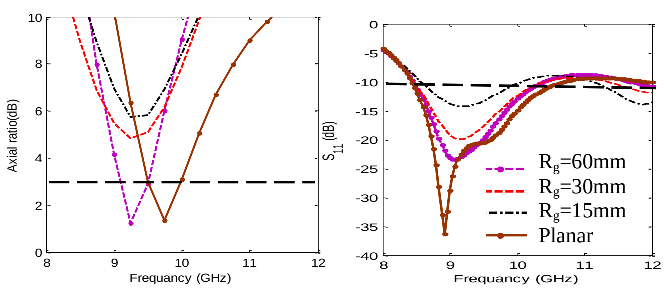

a. The axial ratio. b. The reflection coefficients

Fig.4. The axial ratios and the reflection coefficients versus frequency for different R_g and ψ for fixed l_g and m_g.

Table 1 circular polarization characteristics of DRA mounted on hemi-cylindrical ground plane at different values of R_g and ψ for fixed l_g and m_g.

R_g, ψ	Axial ratio (dB)	CP bandwidth	E_L/E_R
R_g=60 mm ψ = 45°	1.23 dB at f=9.25 GHz	(9.1- 9.51) GH	16.4 dB
R_g=30 mm ψ = 90°	4.82 dB at f=9.25 GHz	----	9.83 dB
R_g=15 mm ψ =180°	5.74 dB at f=9.5 GHz	-----	9.8 dB

To overcome on the degradation of the circular polarization characteristics of the DRA due to the increase in the radius of curvature of the ground plane, the DRA size is modified by varying its height h and the coaxial feeding probe length l_p. The effect of radius of the curvature, R_g, after modification (h, l_p) on the reflection coefficient, axial ratio and the polarization patterns at frequency where the axial ratio is at the minimum of each case are demonstrated in Fig.5. The values of the axial ratio, CP bandwidth and E_L/E_R levels at different radii of curvature are listed in Table II. It is seen that the axial ratio is improved with varying the height of DRA and the length of probe according to the ground radius of curvature. The relationship between the height of the DRA element h for each radius of the hemi-cylindrical ground curvature R_g to get best circular polarization properties is shown in Fig.6. A mathematical representation of this relation is obtained using a curve fitting technique and can be represented by a straight line relation as

$$h = 0.2R_g + 5.5 \quad (1)$$

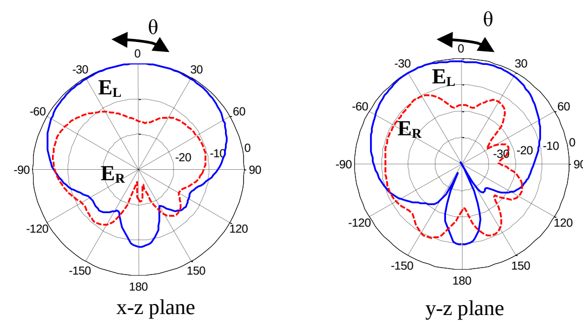

a. R_g=30 mm, h=5.9 mm, l_p=2.9mm

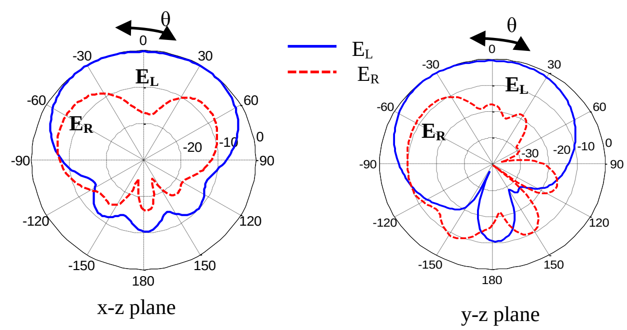

b. R_g=45, h=5.8 mm, l_p=5.8mm

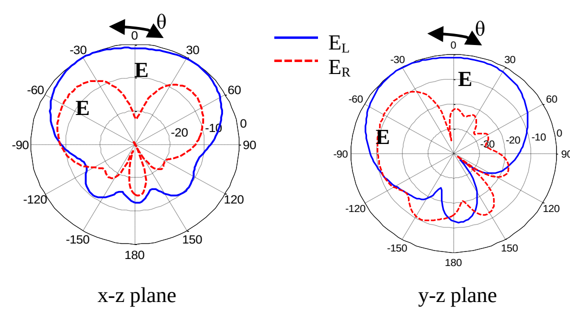

c. R_g=60mm, h=5.6 mm, l_p=5.6

Fig.5. The polarization patterns of DRA for different radii R_g, after modification.

Table II. Comparison of circular polarization characteristics of DRA mounted on hemi-cylindrical ground plane at different values of R_g and ψ for fixed l_g and m_g, after modification, h, l_p.

R_g, ψ	Axial ratio ((dB))	CP bandwidth	E_L/E_R
R_g=60 mm, ψ =45^o h=5.9 mm, l_p=2.9 mm	1.52 dB at f=9.5 GHz	(9.3 -9.75) GHz	21 dB
R_g=45 mm, ψ = 60^o h=5.8 mm, l_p=5.8 mm	2.5 dB at f=9.75 GHz	(9.45 -9.85) GHz	17 dB
R_g=15 mm, ψ = 180^o h=5.6 mm, l_p=5.6 mm	2.45 dB at f=10.25 GHz	(10.15-10.35) GHz	17 dB

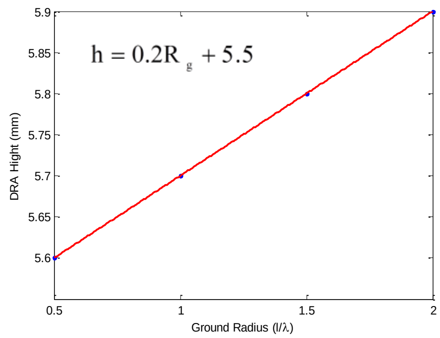

Fig.6. The relation between DRA height and ground plane radius.

B. DRA Element Embedded in a Cylindrical Ground Plane

The previous square DRA element embedded in hemi-cylindrical metallic ground, with a cavity recess height h_c = 7 mm and cavity radius r_c=7 mm, with ground plane radius R_g=30 mm as shown in Fig.7. The simulated reflection coefficient against the frequency and the polarization radiation pattern of the DRA embedded in hemi-cylindrical metallic ground at f= 9.6 GHz are shown in Fig.8. The resonance frequency is shifted up to 9.82 GHz due to the presence of the cavity. The size of DRA does not vary as that happens in case (A). The antenna gives good impedance matching at 9.82 GHz. The impedance matching bandwidth with (S_{11}<-10dB) is 700 MHz. The circular polarization radiation patterns, E_L and E_R, in x-z plane and y-z plane at resonance frequency 9.6 GHz at which the axial ratio has minimum value are shown in Fig.8b. The ratio E_L/E_R=20.13 dB. The FEM method is used to simulate the radiation characteristics of the DRA structure and the results are compared by those calculated by FIT method. Good agreement between the two results methods is obtained.

The effect of radius of curvature, R_g, on the axial ratio, the reflection coefficient, and the circular polarization radiation patterns at the frequency where the axial ratio is at minimum value are demonstrated in Fig.9 and Fig.10. It is seen that the axial ratio is improved by decreasing the radius of the hemi-cylindrical ground plane. When R_g=15 mm the ratio between the circular polarization radiation components at the frequency at which the antenna produces minimum axial ratio value, f=9.82 GHz, is 20.13 dB. The antenna has circular polarization bandwidth (AR<3 dB) over the frequency band from 9.32 GHz to 9.8 GHz within which the antenna matching is still preserved. The impedance matching and resonance frequency are little changed with changing the radius of curvature while the circular polarization patterns nearly the same. Using the embedded cavity, the size of DRA remains constant and not varying by changing R_g. A summary of different cases is presented in Table III.

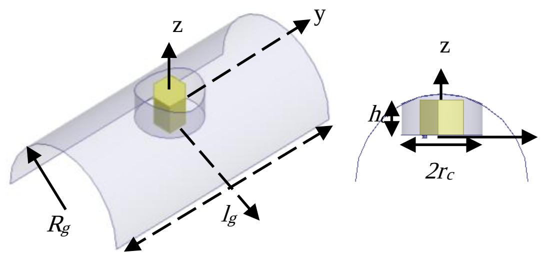

Fig.7. The geometry of DRA element embedded in cylindrical ground plane structure, h_c=7mm, r_c=7mm.

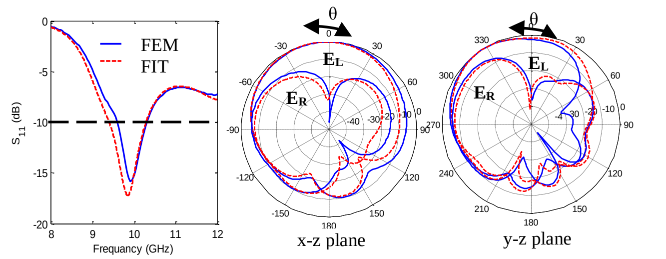

a. Reflection coefficient. b. The polarization radiation patterns at f=9.6 GHz

Fig. 8. The reflection coefficients and the polarization radiation patterns of DRA embedded in cylindrical ground plane, R_g=15 mm, h_c=7 mm, r_c=7 mm.

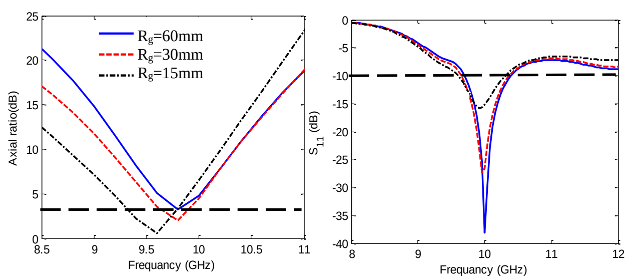

a. The axial ratio *b.* The reflection coefficients.

Fig.9. The axial ratio and the reflection coefficients versus frequency for different radii.

Table:III. . Comparison of circular polarization characteristics of DRA embedded in hemi-cylindrical ground plane at different values of R_g and ψ for fixed l_g and m_g.

R_g	Axial ratio (dB)	CP bandwidth	E_L/E_R
R_g=60 mm and ψ =45^o	3.26 dB at f=9.8 GHz	----	14 dB
R_g=30 mm and ψ =90^o	2.02 dB at f=9.8 GHz	(9.68 - 9.88) GHz	18.69 dB
R_g=15 mm and ψ =180^o	0.5 dB at f=9.6 GHz	(9.32-9.8) GHz	20.13 dB

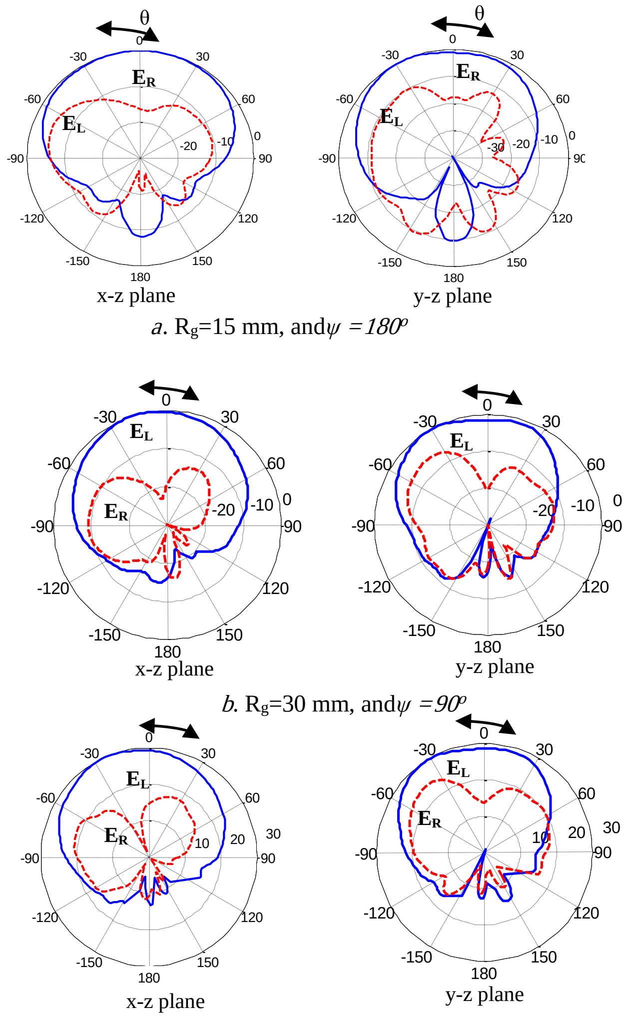

a. R_g=15 mm, and ψ =*180°*

b. R_g=30 mm, and ψ =*90°*

c. R_g=60mm, , and ψ=*45°*

Fig.10. The polarization patterns of DRA for different radii, fixed curvature area after modification.

III. Conclusion

In this paper, the effect of curvature on circular polarization radiation characteristics of the circular polarized DRA element mounted on cylindrical surfaces have been demonstrated. The cylindrical curvature of the surface effects on the size of the DRA element, the DRA structure follows the curvature of the ground plane, and the asymmetry becomes more pronounced. The circular polarization is disappearing with decreasing the radius of curvature (increasing the curvature) where E_L/E_R are deteriorating. To reduce this effect by varying the DRA height *h* and the coaxial feeding probe length l_p to be suitable with the curvature surface. Another solution to overcome the curvature effect on circular polarization characteristics Design embedded structure. This can be achieved by embedding the DRA in a cavity recess in the ground plane in the ground plane. The circular polarization patterns nearly the same with changing the radius of curvature by Using the embedded cavity, the size of DRA remains constant.

IV. References

[1] A. Petosa, Dielectric Resonator Antenna Handbook, Artech House, Inc., Norwood, 2007

[2] Kishk, “Performance of planar four element array of single-fed circularly polarized dielectric resonator antenna,” Microwave and Optical TechnologyLett., vol. 38, no. 5, pp. 381-384, September 2003., 2008.

[3] G. C. Almpanis, Fumeaux, and R. Vahldieck, "The trapezoidal dielectric resonator antenna," IEEE Transactions on Antennas and Propagation, vol.56, no.9, pp. 2810-2816, September 2008.

[4] B. Li, and K.W. Leung, "On the differentially fed rectangular dielectric resonator antenna," IEEE Trans. Antennas Propagate., vol.56, no.2, pp. 353-359, February 2008.

[5] L. a. L. M. S. Ho Sang, "A study on the enhancement of gain and axial ratio bandwidth of the multilayer CP-DRA.," 5th European Conference, 2010.

[6] S. H. Zainud-Deen, H. A. Malhat, and K. H. Awadalla," Dielectric resonator antenna mounted on a circular cylindrical ground plane," Progress In Electromagnetics Research B, PIER B, vol. 19, pp. 427-444, 2010.

[7] S. H. Zainud-Deen, Noha A. El-Shalaby, and K. H. Awadalla," Radiation characteristics of cylindrical dielectric resonator antenna mounted on superquadric cylindrical Body," Electrical and Electronic Engineering Journal, SAP, vol. 2, no. 3, pp.88-95, 2012.

[8] S. H. Zainud-Deen, Noha A. El-Shalaby, and K. H. Awadalla, ," Hemispherical DRA antennas mounted on or embedded in circulFar cylindrical surface for producing omnidirectional radiation pattern" International Journal of Communication, Network and System Sciences, vol.4, no.9, pp. 601-608, September 2011.

[9] S. H. Zainud-Deen, Noha A. El-Shalaby, and K. H. Awadalla," Hemispherical dielectric resonator antenna mounted on or embedded in spherical ground plane with a superstrate," Electrical and Electronic Engineering Journal, SAP, vol. 1, no. 1, pp.5-11, 2011.

[10] S. H. Zainud-Deen, Noha A. El-Shalaby, and K. H. Awadalla," Hemispherical dielectric resonator antennas over non-planar surfaces for direction finding systems," International Journal of Electromagnetics and Applications SAP, vol. 2, no.6, November 2012.

[11] A. Morris, and A. Rahman, A Practical Guide to Reliable Finite Element Modeling, John Wiley & Sons Ltd, The Atrium, Southern Gate, England, 2008.

[12] Mariana Funieru, Simulation of Electromechanical Actuators using the Finite Integration Technique, Ph. D. Thesis, University of Darmstadt, Bukarest, 2007.

[13] I. Munteanu1 and T. Weiland, "RF & Microwave Simulation with the Finite Integration Technique from Component to System Design," Scientific Computing in Electrical Engineering Mathematics in Industry, vo. 11, Part III, pp. 247-260, 2007.